Dynamic Molecular Structure of DPPC-DLPC-Cholesterol Ternary Lipid System by Spin-Label Electron Spin Resonance

Yun-Wei Chiang,* Yuhei Shimoyama,† Gerald W. Feigenson,‡ and Jack H. Freed*
*Baker Laboratory of Chemistry and Chemical Biology, and National Biomedical Center for Advanced Electron Spin Resonance Technology, Cornell University, Ithaca, New York; †Department of Physics, Hokkaido University of Education, Hakodate, Japan; and ‡Department of Molecular Biology and Genetics, Cornell University, Ithaca, New York

ABSTRACT The hydrated ternary lamellar lipid mixture of dipalmitoyl-PC/dilauroyl-PC/cholesterol (DPPC/DLPC/Chol) has been studied by electron spin resonance (ESR) to reveal the dynamic structure on a molecular level of the different phases that exist and coexist over virtually the full range of composition. The spectra for more than 100 different compositions at room temperature were analyzed by nonlinear least-squares fitting to provide the rotational diffusion rates and order parameters of the end-chain labeled phospholipid 16-PC. The ESR spectra exhibit substantial variation as a function of composition, even though the respective phases generally differ rather modestly from each other. The L_α and L_β phases are clearly distinguished, with the former exhibiting substantially lower ordering and greater motional rates, whereas the well-defined L_o phase exhibits the greatest ordering and relatively fast motional rates. Typically, smaller variations occur within a given phase. The ESR spectral analysis also yields phase boundaries and coexistence regions which are found to be consistent with previous results from fluorescence methods, although new features are found. Phase coexistence regions were in some cases confirmed by observing the existence of isosbestic points in the absorption mode ESR spectra from the phases. The dynamic structural properties of the DPPC-rich L_β and DLPC-rich L_α phases, within their two-phase coexistence region do not change with composition along a tie-line, but the ratio of the two phases follows the lever rule in accordance with thermodynamic principles. The analysis shows that 16-PC spin-label partitions nearly equally between the L_α and L_β phases, making it a useful probe for studying such coexisting phases. Extensive study of two-phase coexistence regions requires the determination of tie-lines, which were approximated in this study. However, a method is suggested to accurately determine the tie-lines by ESR.

INTRODUCTION

An extensive variety of lipids constitute the bilayer of biological membranes, but it has in the past been crudely approximated as an homogeneous phase with spatial as well as temporal averaging of the lipid behavior, as in the fluid-mosaic model (Singer and Nicolson, 1972). In fact, this approximation is broken by various physicochemical interactions, e.g., among lipids, ions, and proteins. Heterogeneities in biological membranes are generally poorly characterized in both space and time. The raft model (Simons and Ikonen, 1997) has been one useful way to describe certain bilayer heterogeneities in biomembranes. A more well-defined approach is to characterize model bilayer membranes of binary or ternary mixtures of lipids and cholesterol (Chol) (Brown and London, 1998; Feigenson and Buboltz, 2001).

Feigenson and co-workers have performed extensive studies on a three-component lipid mixture to establish a phenomenological phase diagram (Feigenson and Buboltz, 2001; Huang and Feigenson, 1999). They chose a ternary mixture for which the phase behavior had previously been examined in all three binary mixtures, namely, DPPC/DLPC/Chol. They found that this system manifests ordered, fluid, and coexisting phase regions. To explore the dynamic structure of the various phases at a molecular level for this ternary phase diagram we studied over 100 different ternary mixtures using a spin probe 16-PC, which we found to be particularly sensitive to the different phases. We have been able to establish the ordering and dynamic parameters in these different mixtures, as well as the relative phase amounts in the two-phase regions using ESR simulation methods.

Spin-labeling electron spin resonance (ESR) in conjunction with simulation methods has been a powerful approach in the study of biological membranes and model lipid mixtures (Borbat et al., 2001). The analysis of spectral lineshapes using the microscopic-order macroscopic-disorder (MOMD) model has been shown to yield both dynamic and structural information. In a study of biological membranes, the dynamic structure of detergent-resistant membranes (DRMs) isolated from RBL-2H3 cells has been characterized using two different acyl-chain spin-labeled phospholipids (5PC and 16-PC), a headgroup-labeled sphingomyelin (SM) analog (SD-Tempo), and a spin-labeled cholestane (Ge et al., 1999). More recently, Ge et al. (2003) have found that two phases, a liquid-ordered-like (L_o) and liquid-disordered-like (L_α) phase, coexist in the plasma membrane vesicles prepared from RBL-2H3 mast cells at temperatures ranging from 22°C to 45°C. The effect of aggregation of gramicidin A' on the phase structure of DPPC multilamellar vesicles has been studied by continuous-wave ESR (cw-ESR) using the end-chain-labeled lipid 16-PC at temperatures between 30° and 45°C. Distinctly different spectra were observed from the

Submitted April 14, 2004, and accepted for publication July 22, 2004.

Address reprint requests to Jack H. Freed, Tel.: 607-255-3647; E-mail: jhf@msc.cornell.edu.

0006-3495/04/10/2483/14 $2.00

doi: 10.1529/biophysj.104.044438

bulk lipids and from the boundary lipids that coat the gramicidin A' molecules in the aggregates (Costa-Filho et al., 2003a; Ge and Freed, 1999). A recent study revealed the effects of hydration of the lipid polar headgroup using DPP-Tempo spin-label, and showed that an increase in ordering is correlated with water moving out of the interbilayer region into the bulk water (Ge and Freed, 2003). These studies have shown that ESR spectra provide a powerful tool for investigating the dynamic structure of membranes, including microdomains existing or coexisting in complex membranes.

We also demonstrate that ESR spectra are useful for determining the phase boundaries and phase coexistence in this ternary system. Spectral simulation and fitting using the MOMD model and direct observation of spectral variations in the absorption mode, including the existence of isosbestic points, provides complementary approaches to phase determination, and some new insights pertaining to the ternary phase diagram are obtained.

Very high frequency cw-ESR (Freed, 2000) has great advantages in investigating the subtle aspects of the dynamic structure of membranes (Barnes and Freed, 1998). High frequency (94 GHz) ESR was shown to be very sensitive to lateral lipid-chain ordering in the liquid-ordered phase, upon addition of Chol (Gaffney and Marsh, 1998; Livshits and Marsh, 2000). Use of two distinct microwave frequencies, e.g., 250 GHz and 9.5GHz, facilitates analysis of the dynamic structure of lipid membranes, i.e., L_o versus L_α, in greater detail (Lou et al., 2001). ESR at 250 GHz is more sensitive to the faster dynamic modes, which include internal acyl chain motions, whereas ESR at 9.5 GHz is more sensitive to the slower modes, such as overall lipid motion.

Here we present a dynamic structural view of ternary DPPC/DLPC/Chol mixtures over most of the phase diagram using cw-ESR measurements at 9.5 GHz using multilamellar vesicles. Despite the use of a single ESR frequency at this stage, the extensive range of compositions studied enable us to map out the dynamic structure of this ternary system and to partially characterize and distinguish the various phases, observed at a molecular level.

MATERIALS AND METHODS

Materials

Phospholipids (DPPC and DLPC) and the spin-label 1-palmitoyl-2-(16-doxyl stearoyl) phosphatidylcholine (16-PC), were purchased from Avanti Polar Lipids (Alabaster, AL). Cholesterol was from NuChek Prep (Elysian, MN). Purity >99.5% was established by thin layer chromatography on Adsorbosil Plus 1 silica plates from Alltech Associates (Fairfield, CT) in chloroform/methanol/water = 65/25/4 (vol) for phospholipids and hexane/diethyl ether/chloroform = 7/3/3 for cholesterol. All materials were used without further purification.

Sample preparation and ESR spectroscopy

Measured stock solutions of the lipids in chloroform were mixed in a glass tube. The concentration of spin-label was 0.25 mol % of the lipids. Multibilayer samples were prepared by the method of rapid-solvent exchange (Buboltz and Feigenson, 1999) in a buffer of PIPES/KCl/EDTA = 5 mM/200 mM/1 mM at pH 7.0. Samples were then pelleted using a desktop centrifuge, and transferred to 1.5-mm I.D. capillaries with excess buffer. Samples were deoxygenated in a glove bag by alternately pumping and adding N_2 gas over 3 h. Each capillary was sealed with paraffin.

ESR spectra were obtained on a Bruker Instruments (Billerica, MA) EMX ESR spectrometer at a frequency of 9.55 GHz at room temperature (~24°C).

Stacked plots of ESR absorption spectra

To highlight phase transitions in the phase diagram, we used the absorption mode by integrating the cw-ESR signals. All spectra were normalized to a common area. The baseline was corrected based on the triangular-slope assumption for experimental spectra (Alger, 1968). All plot procedures were performed using MATLAB version 6.5 (The MathWorks, Natick, MA).

NLLS spectral simulations

The dynamic parameters describing the slow-motional regime were obtained from nonlinear least-squares fitting of simulations (Budil et al., 1996) based on the stochastic Liouville equation (Freed, 1976; Freed et al., 1971; Schneider and Freed, 1989).

There are four axis frames used in the simulations: 1), the laboratory frame (X_L, Y_L, Z_L), with its Z axis being defined as the static magnetic field direction; 2), the local director frame (X_d, Y_d, Z_d), which is the bilayer-orienting potential frame fixed in 3), the molecular frame (X_R, Y_R, Z_R), the frame which the rotational diffusion tensor is diagonal; and 4), the magnetic tensor frame (X_m, Y_m, Z_m) in which the g and A tensors are diagonal. $R_\perp$ and $R_\parallel$ are the principal values of an axially symmetric rotational diffusion tensor for the nitroxide moiety attached to the chain segment which characterize the dynamics of the acyl chain.

The K^{th} order parameter of spin-label, S_K, is defined by Polnaszek and Freed (1975) and Schneider and Freed (1989) as

$$S_K \equiv \langle D^2_{0K}(\Omega)\rangle = \int d\Omega\, P_0(\Omega) D^2_{0K}(\Omega), \qquad (1)$$

where the $D^L_{MK}(\Omega)$ are the generalized spherical harmonics, and for $M = 0$, $D^L_{0K}(\Omega) = (4\pi/2L+1)^{1/2} Y_{LK}(\theta,\phi)$, which are the well-known spherical harmonics. S_K is also the K^{th} component of a second-rank traceless irreducible tensor whose symmetry properties are related to those of the potential coefficients, c_{2K} (see below). The $P_0(\Omega)$, given in Eq. 2, is the equilibrium solution to the diffusion equation for a particle undergoing Brownian rotational diffusion in the presence of a potential U:

$$P_0(\Omega) = \exp(-U(\Omega)/kT) / \int d\Omega \exp(-U(\Omega)/kT). \qquad (2)$$

In the principal axis system of a molecular orientation system (taken as the same as that for rotational diffusion) (X_R, Y_R, Z_R), only $\langle D^2_{00}(\Omega)\rangle$ and $\langle D^2_{02}(\Omega) + D^2_{0-2}(\Omega)\rangle$ are nonzero.

The corresponding potential becomes

$$-U(\Omega)/kT = c_{20} D^2_{00}(\Omega) + c_{22}(D^2_{02}(\Omega) + D^2_{0-2}(\Omega)), \qquad (3)$$

or more explicitly

$$U(\Omega) = -kT\left[\frac{c_{20}}{2}(3\cos^2\theta - 1) + c_{22}\left(\sqrt{\frac{3}{2}}\sin^2\theta\cos 2\phi\right)\right], \qquad (4)$$

where $\Omega \equiv (0, \theta, \phi)$, and the angles θ and ϕ are polar and azimuthal angles of the diffusion axis in the local director frame. From Eq. 1 and the forms of Eq. 4, we have order parameters S_0 and S_2 defined in the (X_R, Y_R, Z_R) frame as

$$S_0 \equiv \langle D^2_{00} \rangle = \left\langle \frac{1}{2}(3\cos^2\theta - 1) \right\rangle, \tag{5}$$

$$S_2 \equiv \langle D^2_{02} + D^2_{0-2} \rangle = \left\langle \sqrt{\frac{3}{2}} \sin^2\theta \cos 2\phi \right\rangle, \tag{6}$$

where S_0 is a measure of the extent of alignment of molecular axis Z_R with respect to the local director axis Z_d and S_2 is a measure of the extent to which there is a preferential alignment of the other molecular axes (X_R versus Y_R) with respect to Z_d. It is possible to convert to the principal Cartesian tensor components, since

$$S_{xx} = \frac{1}{2}\sqrt{\frac{3}{2}} S_2 - \frac{1}{2} S_0, \tag{7a}$$

$$S_{yy} = -\frac{1}{2}\sqrt{\frac{3}{2}} S_2 - \frac{1}{2} S_0, \tag{7b}$$

and

$$S_{zz} = S_0. \tag{7c}$$

The spectral simulations for membrane vesicles used in the nonlinear least-squares fittings were obtained with the MOMD model, i.e., the spectra are characterized by lipids in the membrane being microscopically well-aligned within the vesicles, but with macroscopic directors isotropically distributed, so that there is no macroscopic ordering (Meirovitch et al., 1984; Schneider and Freed, 1989).

Spectral-grouping and isosbesticity

ESR absorption spectra, when superimposed, can be grouped according to the type of spectral variation as a function of composition. Abrupt changes in spectral features can signal a phase transition. Normalized absorption spectra should vary continuously with composition within a single phase, and exhibit no well-defined points resembling isosbestic points. A point in an absorption spectrum at which two or more components have the same molar magnetic susceptibility is termed an isosbestic point. It is a point that is invariant to composition as the ratio of components is varied along a tie-line of the phase diagram. In ESR, since the magnetic field is varied, an isosbestic point is observed at a particular magnetic field. The presence of isosbestic points in a group of absorption spectra indicates that two phases coexist in the system in question. The spectral grouping method we use to complement the full spectral analysis is based on these assumptions. The requirement of internal linearity of the system has been discussed for determining the number of components in equilibrium (Brynesta and Smith, 1968; Marriott and Griffith, 1974).

RESULTS

The ternary phase diagram shown in Fig. 1 has been established by Feigenson and Buboltz (2001) for 24°C. All phase definitions have been defined in that article and will be used in the following sections. Samples covering almost the entire 24°C phase diagram were prepared, and their ESR spectra were obtained and fit. They are divided into five series: three having fixed cholesterol concentration, $\chi_{Chol} = 0$, 0.2, or 0.3, and two series having a fixed ratio of DPPC/DLPC = 1/1 or 3/1. A sampling of these extensive spectra is shown in Fig. 2 to illustrate the wide spectral variation and the fits. The rotational diffusion tensor component $R_\perp$ and the order parameter S_0 for 16-PC in DPPC/DLPC/Chol mixtures that we obtained are shown in Fig. 3. These results are shown in a three-dimensional stem plot, wherein the dynamic structure of virtually the entire composition space is mapped out. The cross-section plots for $R_\perp$ and S_0 for each of the five series are shown in Figs. 4–7 to provide a clearer display of the subtle variations of the dynamic parameters in the phase diagram, and they are discussed in the following sections. In addition, we provide equivalent results for the order parameter S_2 in Fig. 8.

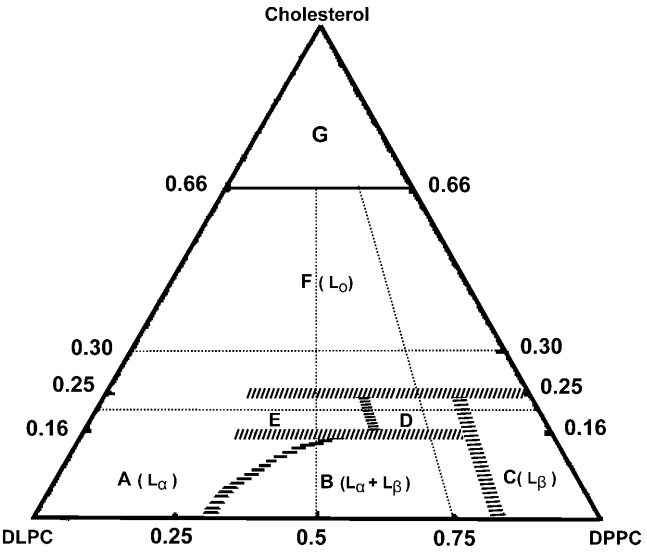

FIGURE 1 Ternary phase diagram for DPPC/DLPC/cholesterol, at 24°C. Each vertex represents a pure component in excess buffer. The numbers labeling the DLPC-DPPC axis correspond to χ^{PC}_{DPPC} whereas the numbers labeling the PC-cholesterol axes correspond to χ_{Chol} and indicate the values associated with various horizontal phase boundaries. Names of phases are marked on the diagram except the *G* region, which is the coexisting crystalline cholesterol monohydrate and a cholesterol-saturated lamellar phase. The *D* and *E* regions are discussed in the text. Five sets of experiments were carried out along five trajectories (*four dotted lines* as well as the *bottom line*) at DPPC/DLPC = 1/1 and 3/1, and $\chi_{Chol} = 0$, 0.2, and 0.3. This phase diagram is from Feigenson and Buboltz (2001).

DPPC/DLPC composition profiles of dynamic parameters at fixed cholesterol ratios

0% cholesterol

We first illustrate our approach with the results for the two-component system corresponding to $\chi_{Chol} = 0$. For binary mixtures of DPPC and DLPC, the two-phase region (Fig. 1, region *B*) is a mixture of DLPC-rich L_α and DPPC-rich L_β

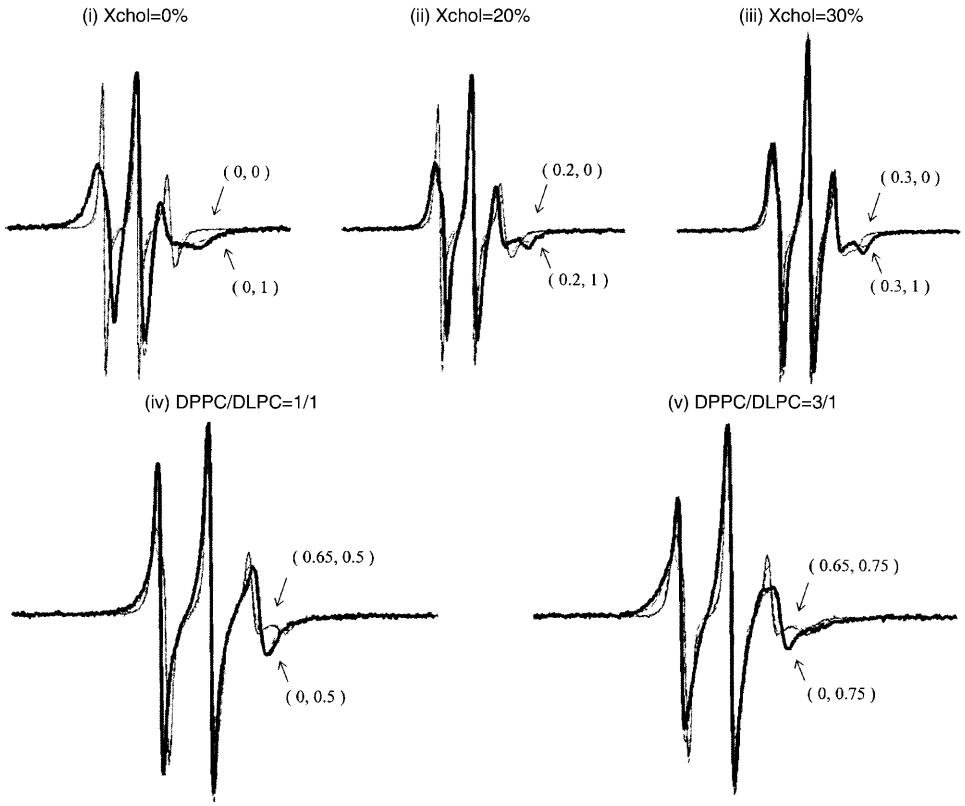

FIGURE 2 The spectra (*solid lines*) and the fits (*dashed lines*) of the two end-points of each trajectory. The composition for respective spectra is marked in the format of (χ_{Chol}, $\chi^{\text{PC}}_{\text{DPPC}}$). The end-chain labeled phospholipid 16-PC exhibits substantially different ESR spectra in the different phases, and it shows considerable ESR lineshape variation with composition.

phases (Feigenson and Buboltz, 2001; Van Dijck et al., 1977). In this two-phase coexistence region, the ESR spectra were fit to an admixture of two spectral components, each with dynamic and ordering parameters corresponding to those of the experimentally determined parameters for the pure spectral component existing at its respective phase boundary. This is consistent with, and a natural consequence of, the requirements of phases in equilibrium. That is, they yield two values of $R_\perp = 1.8$ and $0.7 \times 10^8\ \text{s}^{-1}$ (Fig. 4 *a*) and two values of the order parameter $S_0 = 0.02$ and 0.15 (Fig. 6 *a*) for the end-chain dynamic structure, corresponding to the L_α and L_β phases, respectively. Although these parameters remain constant over the two-phase region, we found that the ratio of the two coexisting phases (for $\chi_{\text{Chol}} = 0$) follows the lever rule (Atkins, 1998) as a function of composition. This implies that the 16-PC spin-label has approximately unity partition coefficient between the L_α and L_β phases, which makes it a good choice for the present study. The partition coefficient K_{P}, the ratio of spin-label concentration in the L_α versus L_β phases, is given by

$$K_{\text{P}} = \frac{[spin\ label\ in\ L_\alpha\ phase]}{[spin\ label\ in\ L_\beta\ phase]} \times \frac{[molar\%\ of\ L_\beta]}{[molar\%\ of\ L_\alpha]}. \quad (8)$$

The first ratio on the right-hand side of Eq. 8 is the ratio of spin-label incorporated in the L_α versus L_β phases from fitting the ESR spectra, and the second is the ratio of mole percentages of L_α versus L_β phases, which is obtained from the lever rule. If the spin-label partitions equally into each coexisting phase, then K_{P} would be unity. We determined K_{P} for 16-PC in the two-phase coexisting region at $\chi_{\text{Chol}} = 0$ over the range of compositions from fitting the ESR spectra. Fig. 9 shows the results from the fits to the ESR spectra versus the lever rule with $K_{\text{P}} = 1$. Numbers shown on the figure are the K_{P} values. The average K_{P} for 16-PC in the region is 0.88 ± 0.24.

Phase coexistence along the $\chi_{\text{Chol}} = 0$ trajectory, which is necessarily along a tie-line, may be confirmed even without spectral simulation by observing the presence of isosbestic points (see Fig. 10 *A*). After normalizing the areas of the absorption spectra, we plotted them together and found that the spectra with $\chi_{\text{Chol}} = 0$ can be divided into three groups based on their respective lineshapes. Isosbestic points are found only in the spectra from the two-phase region. The spectra in the two 1-phase regions, $\chi^{\text{PC}}_{\text{DPPC}} = 1.0 \sim 0.85$ and $0.3 \sim 0$, vary continuously and smoothly with no appearance of isosbestic points. In the spectral analysis we find continuous variation in $R_\perp$ (see Fig. 4 *a*) and S_0 (see Fig. 6 *a*) in these regions. We do observe a relatively abrupt change (shown in Fig. 10 *A i*) between the spectrum of pure DPPC ($\chi^{\text{PC}}_{\text{DPPC}} = 1$) and the spectrum of the mixture, $\chi^{\text{PC}}_{\text{DPPC}} = 0.95$. On the basis of the characteristic wide-angle x-ray diffraction pattern (Tardieu et al., 1973), it is well-known that $\chi^{\text{PC}}_{\text{DPPC}} = 1$ is the $L_{\beta'}$ (tilted gel) phase at this temperature. We thus interpret this as ESR spectral evidence, found for the first time, that pure DPPC is in the $L_{\beta'}$ phase

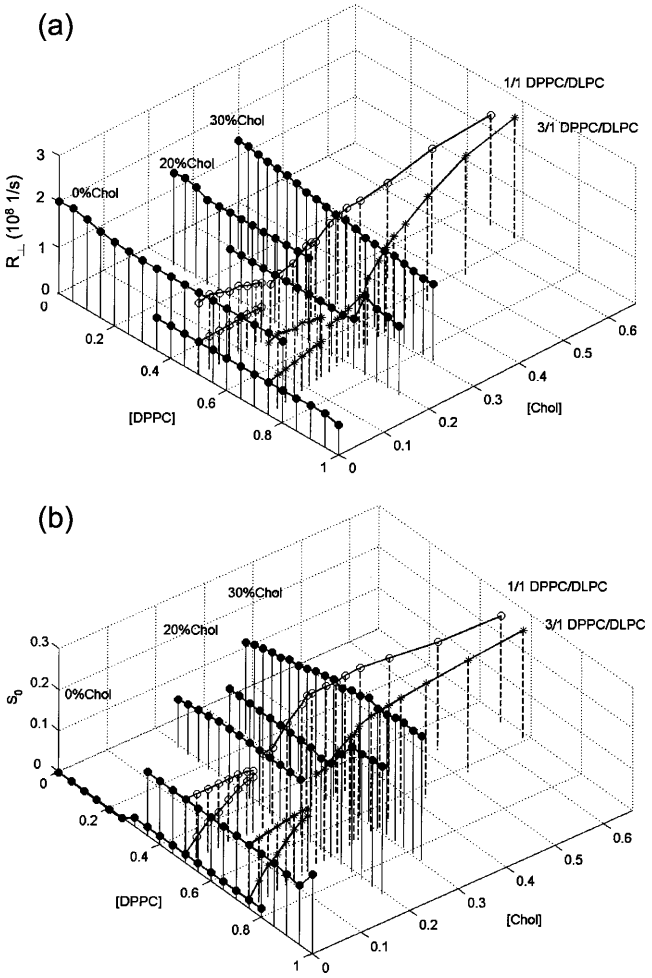

FIGURE 3 Three-dimensional stem plots of ESR fitting results. (*a*) Rotational diffusion rates $R_\perp$ and (*b*) order parameters S_0 for 16-PC in DPPC/DLPC/Cholesterol mixtures.

converting to the L_β phase at $\chi^{PC}_{DPPC} = 0.95$. In the spectral analysis, this shows up as a sharp inflection point in S_0 (see Fig. 6 *a*) and a weaker one in $R_\perp$ (see Fig. 4 *a*) at this composition. The isosbesticity analysis was employed as complementary to the ESR spectral simulations, as well as to the previous studies of this phase coexistence (Feigenson and Buboltz, 2001), as discussed below in more detail.

20% cholesterol

The dynamic parameters for $\chi_{Chol} = 0.2$ series are shown in Fig. 4 *b* for $R_\perp$ values and Fig. 6 *b* for S_0 values. Along the composition trajectory $\chi_{Chol} = 0.2$ as the concentration of DPPC increases, S_0 increases slightly from 0.11 at $\chi^{PC}_{DPPC} = 0$ to $S_0 = 0.13$ at $\chi^{PC}_{DPPC} = 0.2$. Related changes were found in the $R_\perp$ values (Fig. 4 *b*), which decreased slightly from 0.2 to 0.18 $\times$ 10^9 s^{-1} over the region. These results show gradual changes in the L_α phase over this one-phase region, but also uncover a new boundary in the phase diagram. The region $\chi^{PC}_{DPPC} = 0.25 \sim 0.6$ appears to be a two-phase coexistence region (shown by *solid lines* in Figs. 4 *b* and 6 *b*), since presumed isosbestic points are observable (see Fig. 10 *B iii* and below) in addition to the simulation and fitting of the ESR spectra. However, the spectra in this region were analyzed with an assumed horizontal tie-line. Oddly, in this case we found that the fits with the two spectral components from each end of the assumed tie-line do not show improved quality of fit as compared to the one-component fits. This could, in part, be due to the fact that the spectra in this region only change modestly with composition. In addition, it could be that the true tie-lines in this region are actually at a substantial angle with respect to the assumed horizontal tie-line. But, if this is the case, we would not expect well-defined isosbestic points. (Clearly one must be careful in assigning isosbestic points to regions where there is not substantial change in the ESR spectra with composition.) The single spectral component fit is also shown in Figs. 4 *b* and 6 *b* as dashed lines. Proper investigation of tie-lines in this region would require making extensive samples along the boundaries, then using their spectra as basis spectra for systematically studying the two-component region. Just above $\chi^{PC}_{DPPC} = 0.65$, there is a transition to a composition region where $R_\perp$ remains constant, while S_0 increases somewhat more rapidly to 0.28 at $\chi^{PC}_{DPPC} = 0.8$ (Fig. 6 *b*). Further increase in DPPC concentration shows a transition to the L_β phase with $R_\perp$ nearly doubling to 0.17 $\times$ 10^9 s^{-1} without much change in S_0 in crossing the boundary at $\chi^{PC}_{DPPC} = 0.85$.

The ESR absorption spectra of $\chi_{Chol} = 0.2$ are shown in Fig. 10 *B*. The spectra with $\chi_{Chol} = 0.2$ are divided into four categories by observing the differences in the stacked

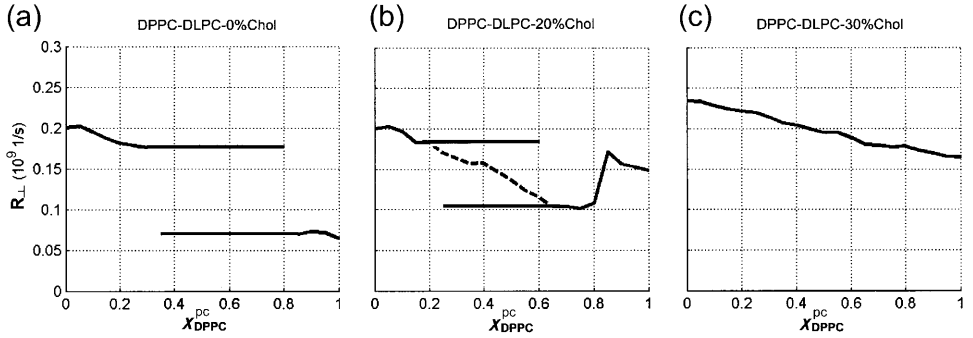

FIGURE 4 The cross-section plots of rotational diffusion rates $R_\perp$ from the ESR fitting for the series of (*a*) $\chi_{Chol} =$ 0, (*b*) 0.2, and (*c*) 0.3. Two $R_\perp$ values for a given χ^{PC}_{DPPC} value imply a two-phase coexistence region. The $R_\perp$ of the L_α phase is approximately two-times faster than that in the L_β phase. The results of a one-component fit are shown by a dashed line.

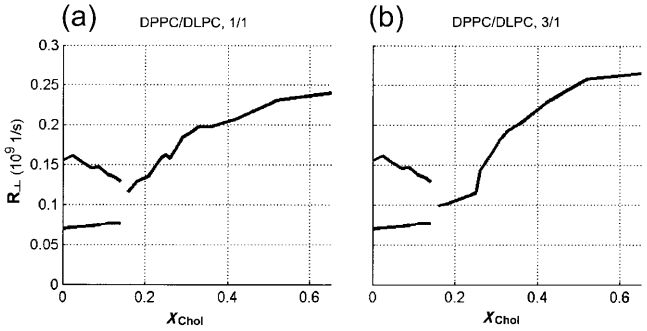

FIGURE 5 The cross-section plots of rotational diffusion rates $R_\perp$ from the ESR fitting for the series of (*a*) DPPC/DLPC = 1/1 and (*b*) 3/1. Two $R_\perp$ values for a given χ_{Chol} value imply a two-phase coexistence region.

absorption spectra. The boundaries associated with the four categories are consistent with the simulation results from the NLLS fitting program, which imply four different regions along the composition trajectory with $\chi_{Chol} = 0.2$. We have already discussed (apparent) isosbestic points for the region $\chi^{PC}_{DPPC} = 0.25{\sim}0.6$ shown in Fig. 10 *B iii*. Similar comments apply to the (apparent) isosbestic points for the region $\chi^{PC}_{DPPC} = 0.65{\sim}0.8$ shown in Fig. 10 *B ii*. Previously, we described these regions as a liquid-ordered phase (Fig. 1 *E*) from $\chi^{PC}_{DPPC} = {\sim}0.25{\sim}0.6$ that changes to a rigid-ordered phase over 0.65 ~0.8 (Fig. 1 *D*) (Feigenson and Buboltz, 2001). However, our ESR results suggest phase coexistence in these regions. The regions $\chi^{PC}_{DPPC} = 0{\sim}0.2$ and $0.85{\sim}1$ show no evidence for more than one phase, by the clear absence of isosbestic points, and by the spectral simulation results.

We tentatively assign the region $\chi^{PC}_{DPPC} = {\sim}0.25{\sim}0.6$ as an admixture of L_α phase, which exists as a single phase for $\chi^{PC}_{DPPC} = 0{\sim}0.2$, and an L_o phase. The latter is characterized by an S_0 that is approximately double that of the L_α phase and an $R_\perp$ that is almost half. Given the limited data, we did not attempt to fit the spectra for the region $\chi^{PC}_{DPPC} = 0.65{\sim}0.8$ with two spectral components; instead the best one-component fit corresponds to a phase of high order together with significant mobility. This is a complex region of the phase diagram, clearly warranting further study.

30% cholesterol

Along the composition trajectory $\chi_{Chol} = 0.3$, both the spectral fitting (compare to Figs. 4 *c* and 6 *c*) as well as the spectral grouping method (Fig. 10 *C*) show no evidence of more than one phase. $R_\perp$ decreases slightly from 0.23×10^9 s^{-1} at $\chi^{PC}_{DPPC} = 0$ to 0.16×10^9 s^{-1} at $\chi^{PC}_{DPPC} = 1$, whereas S_0 gradually increases from 0.22 at $\chi^{PC}_{DPPC} = 0$ to 0.3 at $\chi^{PC}_{DPPC} = 0.7$, and then levels off above $\chi^{PC}_{DPPC} = 0.7$. By plotting the ESR absorption spectra, the one-phase region was further supported because no isosbestic points appear in the stacked spectra. (That is, although there is crossover in the high-field region of the spectrum shown in Fig. 10 *C*, this is not at a single distinct point but varies with composition. The simulations confirm that this is due to lineshape changes resulting from slow-motional effects.) Since this is a region of substantial S_0 and relatively large $R_\perp$ it is appropriately characterized as an L_o phase, as previously proposed (Feigenson and Buboltz, 2001).

Cholesterol composition profiles of dynamic parameters at fixed DPPC/DLPC ratios

For the composition trajectories at fixed molar ratios DPPC/DLPC = 1/1 and 3/1, with varying cholesterol concentrations from $\chi_{Chol} = 0.0$ ~0.65, there are three major findings shown in the NLLS simulation results. The cross-section plots of $R_\perp$ and S_0 values for the series, DPPC/DLPC = 1/1 and 3/1, are shown in Figs. 5 and 7, respectively. Since there are many common features, we consider them jointly and comment, when appropriate, on the differences.

First of all, the spectra of samples in the $L_\alpha + L_\beta$ region were fit with two spectral components with their respective sets of parameters. The component spectra should correspond to compositions at the boundaries around the region. That is, a spectrum of a given composition in the $L_\alpha + L_\beta$ region must be the superposition of the two spectra obtained at the ends of the tie-line associated with that composition. Then one expects that the NLLS fitting would yield a phase ratio that is consistent with the lever rule and the partition coefficient of the probe (compare to Eq. 8). We took the tie-lines in the $L_\alpha + L_\beta$ region lines to be parallel to the bottom

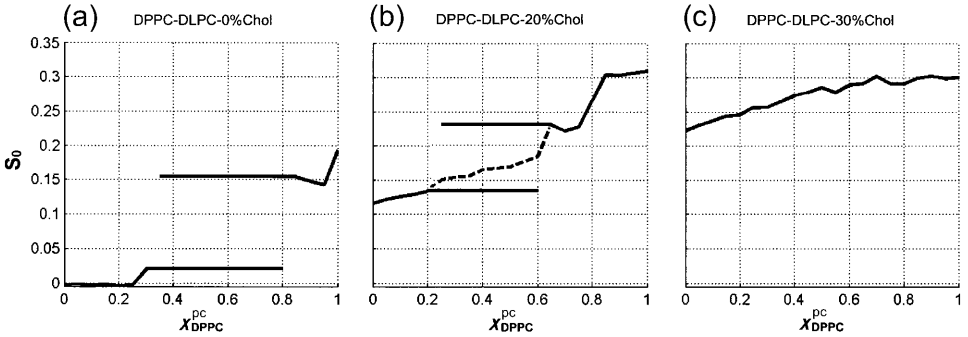

FIGURE 6 The cross-section plots of order parameters S_0 from the ESR fitting for the series of (*a*) $\chi_{Chol} = 0$, (*b*) 0.2, and (*c*) 0.3. Two $R_\perp$ values for a given χ^{PC}_{DPPC} value imply a two-phase coexistence region. The results of a one-component fit are shown by a dashed line.

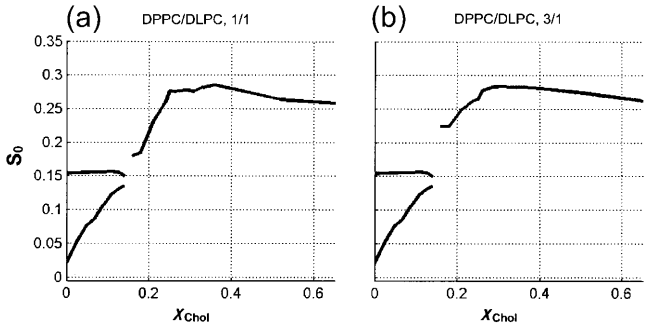

FIGURE 7 The cross-section plots of order parameters S_0 from the ESR fitting for the series of (*a*) DPPC/DLPC = 1/1 and (*b*) 3/1. Two $R_\perp$ values for a given χ_{Chol} value imply a two-phase coexistence region.

horizontal line (0% Chol) of the phase diagram, which we already noted, is necessarily a tie-line for the two-component DPPC/DLPC system. Indeed we found that the composition ratios in the *B* (L_α + L_β) region returned from the NLLS fitting program are consistent with those calculated from the lever rule. This also indicates that 16-PC spin-label partitions approximately equally between the DPPC-rich and DLPC-rich phases even in the presence of cholesterol. In addition, the spectral component fits yielded the dynamic structures of boundaries around this region. As χ_{Chol} increases from 0 to 0.16, the order parameter S_0 at the boundary of the DLPC-rich region (Fig. 7) dramatically increases from 0.02 to 0.13, whereas that of the boundary of the DPPC-rich region remains almost constant at 0.15. The corresponding $R_\perp$ values in the same region (Fig. 5) were found to decrease slightly from 0.15 to 0.13 $\times$ 10^9 s^{-1} for the DLPC-rich spectral component, and remain virtually constant at 0.07 $\times$ 10^9 s^{-1} for the DPPC-rich component. The dynamic structure of the two boundaries among L_α, L_α + L_β, and L_β regions is thus rigorously characterized by the ESR spectral fitting method.

Secondly, the boundaries at the top and bottom of regions *E* (for DPPC/DLPC = 1/1) and *D* (for DPPC/DLPC = 3/1; see Fig. 1) are confirmed by observing changes in both $R_\perp$ and S_0. A large jump in S_0 was observed as χ_{Chol} crosses over the boundary from the *B* to the *D* region (at $\chi_{Chol} \sim 0.15$). In the *D* region, the $R_\perp$ and S_0 increase in a way that is totally different from the behavior of the dynamic parameters in the *B* and *E* regions. In the *E* region, the change in S_0 is dramatically sharp, which increases from 0.18 at χ_{Chol} = 0.16 to 0.27 at $\chi_{Chol} = 0.3$. The evidence of the boundaries at $\chi_{Chol} = 0.16$ and 0.25 is of significance since the dynamic structures of *B*, *D*, *E*, and *F* revealed by ESR simulation results are different. However, we must caution the reader that the *D* and *E* regions are likely composed of (at least) two phases (see above), but the limited data available precluded us from trying to fit the results to more than one ''average'' phase.

Thirdly, S_0 dramatically increases in the *E* and *D* regions from $\chi_{Chol} = 0.16$ to that at $\chi_{Chol} = 0.25$, whereas it levels off beyond $\chi_{Chol} = 0.25$ and almost plateaus beyond χ_{Chol} = 0.3. This indicates that at the higher χ_{Chol}, the effect of cholesterol concentration on the ordering in the lipid membranes is saturating, but the rotational diffusion rate of spin-labels does increase in the liquid-ordered phase. This phenomenon may be a general characteristic of the L_o phase, which emerges from the present study where many different compositions were examined.

The absorption spectra of DPPC/DLPC = 1/1 with χ_{Chol} varying from 0.0 to 0.65 are shown in Fig. 11. The most obvious characteristic of the series is that the high-field edge of the high-field peak appears to split. This feature may be used as a criterion to help separate these spectra into three categories: $\chi_{Chol} = 0 \sim 0.13$ and $0.24 \sim 0.65$, wherein there is a distinct single high-field peak, and the middle category, $\chi_{Chol} = 0.14 \sim 0.21$ (Fig. 11 *ii*). This is consistent with the existence of two boundaries located somewhere between $\chi_{Chol} = 0.13 \sim 0.14$ and $\chi_{Chol} = 0.21 \sim 0.24$, respectively. Isosbestic points are not at all clear in the region of Fig. 11 *i*, nor should they be, since this series represents composition changes that do not occur along a single tie-line. This is because the individual component spectra are themselves changing with composition, so, along the trajectory followed, the composite spectra are no longer a simple linear combination of the same component spectra. This accounts for why we clearly see isosbestic points in the χ_{Chol} = 0 series, but not in the DPPC/DLPC = 1/1 (see Fig. 11) and 3/1 series (not shown, since the absorption spectra changes in this series are similar to the DPPC/DLPC = 1/1). Also, no isosbestic point was seen in Fig. 11 *ii*, which is tentatively observed as a two-phase region in the χ_{Chol} = 0.2 series, probably due in part to too few spectra (only three) to show isosbestic points in this narrow region.

Absorption spectra of the DPPC/DLPC = 3/1 series with χ_{Chol} varying from 0.0 to 0.65 could be characterized by the three groupings with regions corresponding to those found in the DPPC/DLPC = 1/1 series. The evidence for boundaries existing at the top and bottom of the *D* region is clear, since 1), the series, DPPC/DLPC = 1/1 and 3/1, show the same boundaries and 2), the biggest changes in the dynamic parameters from the spectral fits occur as the sample composition crosses these two boundaries.

Ordering tensor

We have so far for simplicity in presentation, not referred to the results in Fig. 8 on the order parameter S_2, which measures the asymmetry in the alignment of the nitroxide at the end of the acyl chain. For example, we see in Fig. 6 *a* (0% Chol) that for DLPC-rich mixtures, wherein $\chi^{PC}_{DPPC} < 0.25$, S_0 is negligibly small, which by itself implies no ordering. However, Fig. 8 *B i* shows substantial negative values of S_2, and using the expressions in Eq. 7, we find, for example, for pure DLPC ($\chi^{PC}_{DPPC} = 0$), $S_{xx} = -0.153$, $S_{yy} = 0.155$, and $S_{zz} = -0.0026$. Thus there is substantial positive alignment

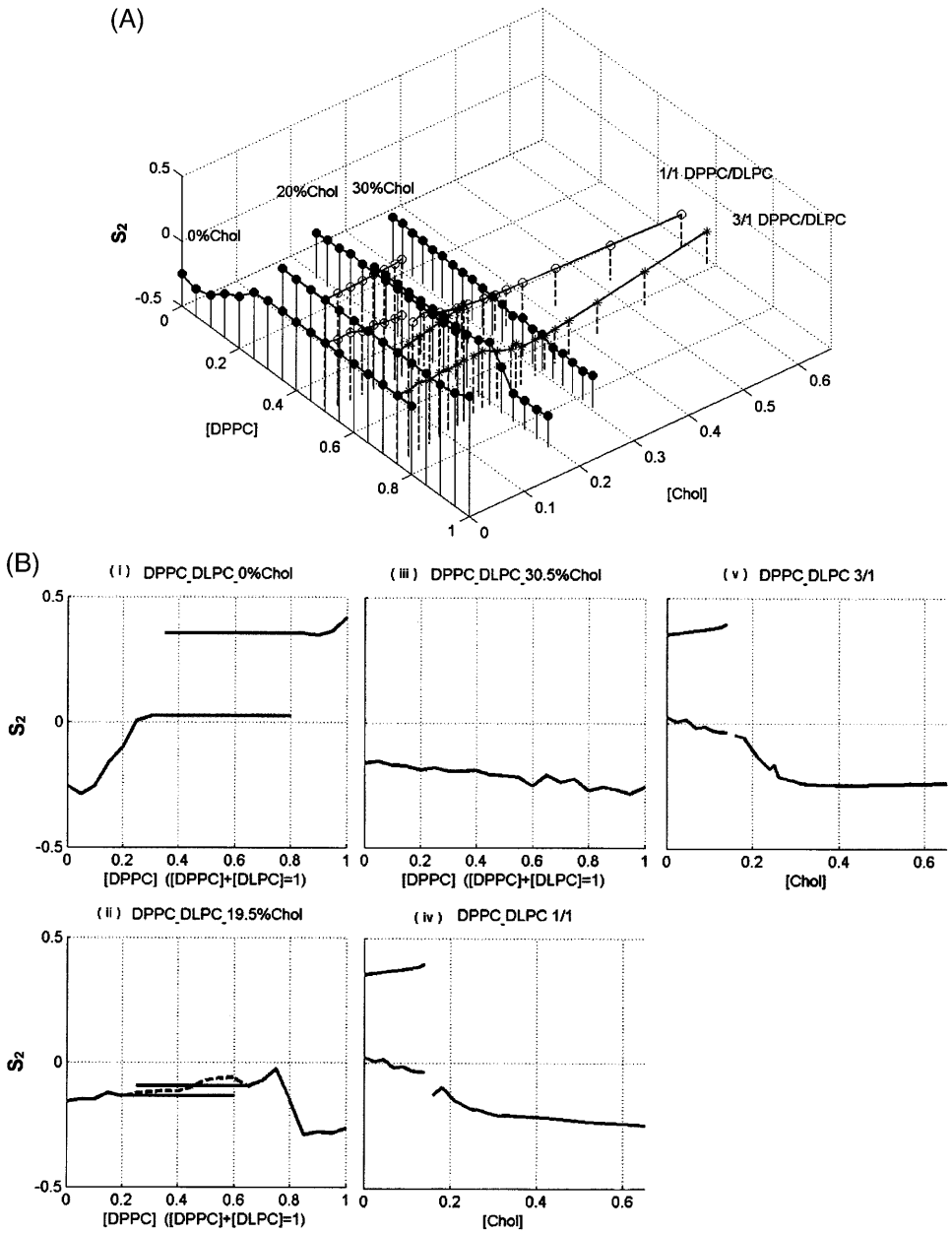

FIGURE 8 The order parameter S_2: (*A*) 3D stem plot and (*B*) the cross-section plots of the respective trajectories. It shows the asymmetry in the alignment of the nitroxide at the end of the acyl chain (see Eq. 7).

of the nitroxide *y* axis relative to the membrane normal, even though the alignment of the nitroxide *z* axis is negligible. A positive *y* alignment is consistent with tilting of the end of the hydrocarbon chain, as would be expected from a label at the 16-carbon position, given the lauroyl acyl chain is only 12 carbons long. (An analogous feature has been observed when a 16-PC molecule coats the shorter gramicidin A peptide; Costa-Filho et al., 2003a.) However, addition of DPPC, with its 16-carbon acyl chains, appears to remove this feature. Thus for $\chi^{PC}_{DPPC} = 0.3$ and $\chi_{Chol} = 0$ one finds $S_{xx} = 0.004$, $S_{yy} = -0.02$, and $S_{zz} = 0.024$, corresponding to almost negligible *y* ordering. On the other hand, the transition from $L_{\beta'}$ to L_β phase that occurs at $\chi^{PC}_{DPPC} = 0.95$ noted above shows up as an increase in S_2. The resulting tensor components are for $\chi^{PC}_{DPPC} = 1.00$: $S_{xx} = 0.16$, $S_{yy} = -0.35$, and $S_{zz} = 0.19$; and for $\chi^{PC}_{DPPC} = 0.95$: $S_{xx} = 0.15$, $S_{yy} = -0.29$, and $S_{zz} = 0.14$, which reflects a somewhat reduced ordering tensor. In the L_o phase the ordering tensor changes only slightly with composition (see Figs. 6 *c*, 7, and 8 *B iii–v*) and it corresponds to $S_{yy} \approx 0$ throughout (e.g., $S_{xx} = -0.27$, $S_{yy} = 0.01$, and $S_{zz} = 0.26$ for $\chi_{Chol} = 0.52$ and $\chi^{PC}_{DPPC} = 0.5$), which is different in character from the previous examples. This feature of $S_{yy} \approx 0$ also characterizes the effect of addition of cholesterol ($\chi_{Chol} = 0.2$) to the L_α and L_β phases even though the overall ordering varies considerably; see Figs. 6 *b* and 8 *B ii* (e.g., for $\chi^{PC}_{DPPC} = 0$, one has $S_{xx} = -0.16$, $S_{yy} = 0.04$, and $S_{zz} = 0.12$; and for $\chi^{PC}_{DPPC} = 1.0$, one has $S_{xx} = -0.32$, $S_{yy} = 0.007$, and

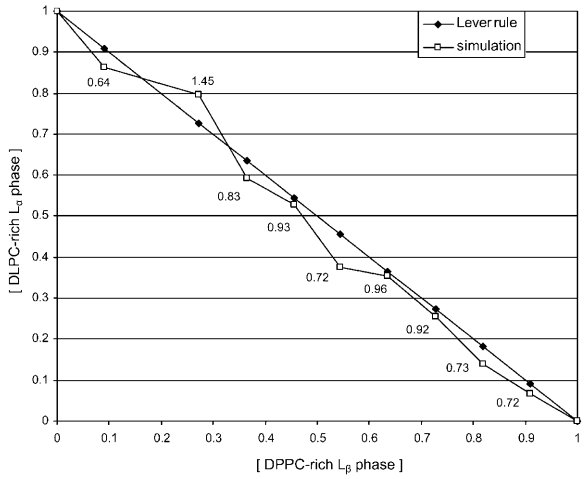

FIGURE 9 Correlation plots for the partition ratios of 16-PC in the DPPC-rich and DLPC-rich coexisting regions for the $\chi_{Chol} = 0$ series. It shows the results from the fits to the ESR spectra versus the lever rule with partition coefficient $K_P = 1$. The best-fit K_P values are marked on the plot. The average K_P for 16-PC in the region is 0.88 ± 0.24, indicating that the spin-probe partitions in equal concentration between the two coexisting phases.

$S_{zz} = 0.31$). A value of $S_{yy} \approx 0$ could be a consequence of the nitroxide *y* axis being preferentially tilted at or near the magic angle (54.7°) with respect to the membrane normal. One must be careful, however, with detailed interpretations of the ordering that arises from the MOMD analysis, a matter we consider in Discussion, below.

DISCUSSION

Dynamic structure of ternary lipid system

The principal objective of this study has been to provide insight at the molecular level of the dynamic structure of the various phases of the DPPC/DLPC/Chol ternary system which was previously characterized phenomenologically. Our study has provided insight into the dynamics and ordering sensed by a spin-label located at the end of the acyl chain (16-PC). This has proved to be a useful probe both because it shows considerable ESR lineshape variation with composition, which can then be analyzed in terms of changes in dynamics and ordering at the chain end, and also because it is found to partition approximately equally between the DLPC-rich L_α phase and the DPPC-rich L_β phase, so phase coexistence can be discerned in two separate phase regions. Overall it must be said that the respective phases, as viewed from close to the center of the bilayer, show fairly gentle differences in ordering and dynamics, emphasizing that these phases, although distinct, are not so markedly different. Thus it is important to have a methodology that is sensitive to such distinctions.

The L_α and L_β phases that exist and coexist for low cholesterol content mixtures are well distinguished in terms of the very low ordering of the former and appreciable ordering and reduced motion of the latter. Addition of cholesterol would appear to enhance ordering in the L_α phase without appreciably modifying the motional rate. The phase in region *E* (see Fig. 1) that appears to coexist at 20 mol % cholesterol with the L_α phase, shows a substantially greater ordering and somewhat reduced motion than the L_α phase, as would be expected, but further addition of DPPC converts it to the L_β phase with both enhanced ordering and motional rates, a feature normally regarded as characteristic of liquid-ordered phases. (Note that these considerations suggest that region *D* may consist of three coexisting phases, but this is a matter for further study.) However, higher cholesterol content of 30% or greater does lead to characteristic liquid-ordered phase behavior, namely relatively large ordering and high motional rate.

According to Fig. 1 as well as to our ESR results on the phase boundaries, a trajectory of increasing cholesterol concentration coming at $\sim\chi^{PC}_{DPPC} = 0.2$ would involve no phase transitions, but would continuously go from the L_α phase to the L_o phase, passing through a supercritical region. Our results show this, where the ordering grows gradually from near zero to the high levels of the L_o phase, while the diffusional rates remain relatively large with perhaps only a small increase. In this sense the L_α phase we are nominally ascribing to the 20% cholesterol trajectory (e.g., region *E*) might be the supercritical form of L_α and L_o phases. One might further speculate that the phase in coexistence in region *E* with this presumed supercritical phase, is itself an L_o phase that emerges from the DPPC-rich L_β phase as cholesterol is added. Only with appreciable cholesterol ($\chi_{Chol} > 0.25$) would this latter L_o phase be indistinguishable from that of the region *F*, which appears to be a ''dominant'' L_o phase. These suggestions could be studied further, and possibly confirmed, by the use of additional spin-probes, such as was used in a recent 2D-ELDOR study of the L_α versus L_o phases in the binary DPPC/Chol system (Costa-Filho and Freed, 2003; Costa-Filho et al., 2003b). There, in addition to 16-PC, a headgroup-labeled lipid probe and a labeled cholesterol analog were used, providing further insight into the differences between the two phases. Another virtue of the 2D-ELDOR method is its enhanced sensitivity to the dynamic structure of lipid membranes in these phases despite their quite subtle differences.

Relation to previous studies

ESR has in the past been used to study lateral phase separation in model membranes (McConnell, 1976; Recktenwald and McConnell, 1981; Shimshick and McConnell, 1973; Shin and Freed, 1989a,b; Veiga et al., 2001; Wolf and Chachaty, 2000). The results obtained by ESR were found to be in generally good agreement with complementary studies by other physical methods, such as fluorescence recovery after photobleaching (Rubenstein et al., 1979), freeze-fracture transmission electron microscopy (Kleemann and

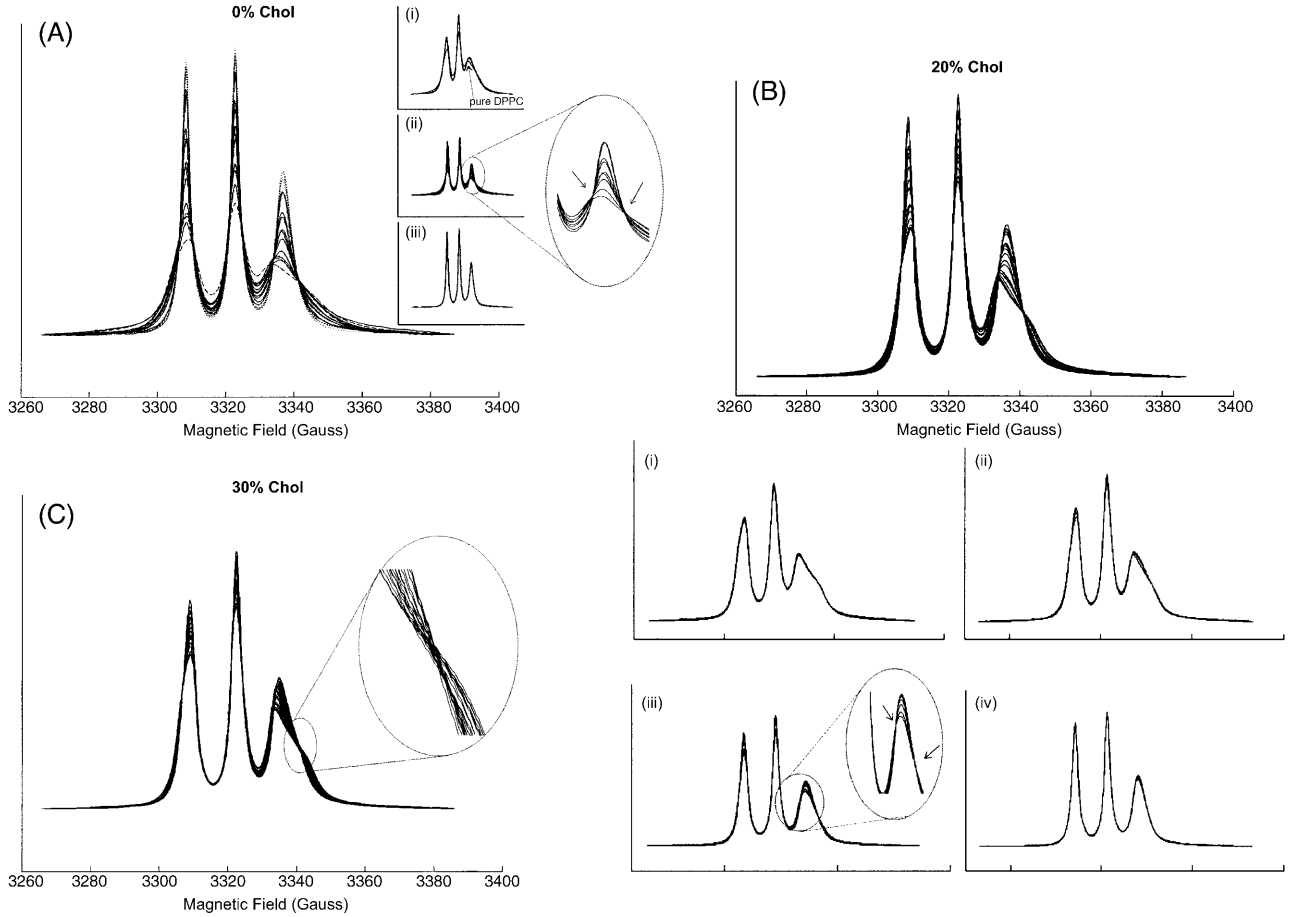

FIGURE 10 (*A*) The absorption ESR spectra for the $\chi_{Chol} = 0$ series. χ^{PC}_{DPPC} is varied from 1.0 to 0 with intervals of 0.05 (note $\chi^{PC}_{DPPC}+\chi^{PC}_{DLPC} = 1.0$.) These spectra exhibit three groups, which are shown in the inserts on the right side. (*i*) The spectra of $\chi^{PC}_{DPPC} = 1.0$ to 0.85 (*dashed lines*). Each spectrum varies smoothly with respect to the different concentrations of DPPC and DLPC, indicating this is a one-phase region. (*ii*) There are two isosbestic points (*marked*) shown in the range of $\chi^{PC}_{DPPC} = 0.8$ to 0.35 (*solid lines*), indicating the DLPC-rich fluid lamellar phase and DPPC-rich order phase are coexisting, which is consistent with FRET results (compare to Feigenson and Buboltz, 2001). (*iii*) The range of $\chi^{PC}_{DPPC} = 0.3$ to 0 (*dotted lines*). This is a one-phase region with no isosbestic points. (*B*) The absorption ESR spectra for the $\chi_{Chol} = 0.2$ series. χ^{PC}_{DPPC} are varied from 1.0 to 0 with an interval of 0.05 ($\chi^{PC}_{DPPC}+\chi^{PC}_{DLPC} = 1.0$.) Spectra in this series could be divided into four groups. They represent respectively $\chi^{PC}_{DPPC} =$ (*i*) $1.0 \sim 0.85$, (*ii*) $0.8 \sim 0.65$, (*iii*) $0.6 \sim 0.25$, and (*iv*) $0.2 \sim 0$, which indicates there are four phase regions along this series. Apparent isosbestic points (*marked*) in region *ii* suggest there are two phases coexisting. (*C*) The absorption spectra for the $\chi_{Chol} = 0.3$ series. χ^{PC}_{DPPC} is varied from 1.0 to 0 with an interval of 0.05 (note $\chi^{PC}_{DPPC}+\chi^{PC}_{DLPC} = 1.0$.) Overall spectra in this series vary pretty smoothly and continuously. This result confirms that one phase changes continuously in this fluid-ordered region.

McConnell, 1976), nuclear magnetic resonance and differential scanning calorimetry (Vist and Davis, 1990), quasielastic neutron scattering (Gliss et al., 1999), and small angle x-ray scattering (Wolf et al., 2001).

ESR has also been particularly useful in studying the dynamic structure of model membranes (Barnes and Freed, 1998; Borbat et al., 2001; Cassol et al., 1997; Ge et al., 1994; Kar et al., 1985; Lou et al., 2001; Shin et al., 1993, 1990; Shin and Freed, 1989a; Tanaka and Freed, 1984), providing insight into the L_α, L_β, and L_o phases. It provides motional rates as well as ordering. The well-known cholesterol-condensing effect on membranes (Demel et al., 1967; Leathes, 1925; Stockton and Smith, 1976; Vist and Davis, 1990), which involves increase in acyl-chain order parameter (Aussenac et al., 2003; Miao et al., 2002; Pare and Lafleur, 1998), is clearly demonstrated in the ESR studies. As noted above, a more advanced form of ESR, 2D-ELDOR, is particularly sensitive to the subtle details of the dynamic structure of membranes (Borbat et al., 2001; Costa-Filho et al., 2003b; Crepeau et al., 1994).

This present ESR study is unique in addressing the full ternary phase diagram, although some past ESR studies dealt with partial exploration of three (or more) component model membranes including cholesterol (Shin et al., 1993; Veiga et al., 2001; Wolf and Chachaty, 2000). As a result, this study has demonstrated the subtle, but distinct features on a molecular level, which characterize the various phases that can exist in model membranes. Our present results can most directly be compared with past ESR studies on the DPPC/Chol binary system using 16-PC. In fact, we find excellent

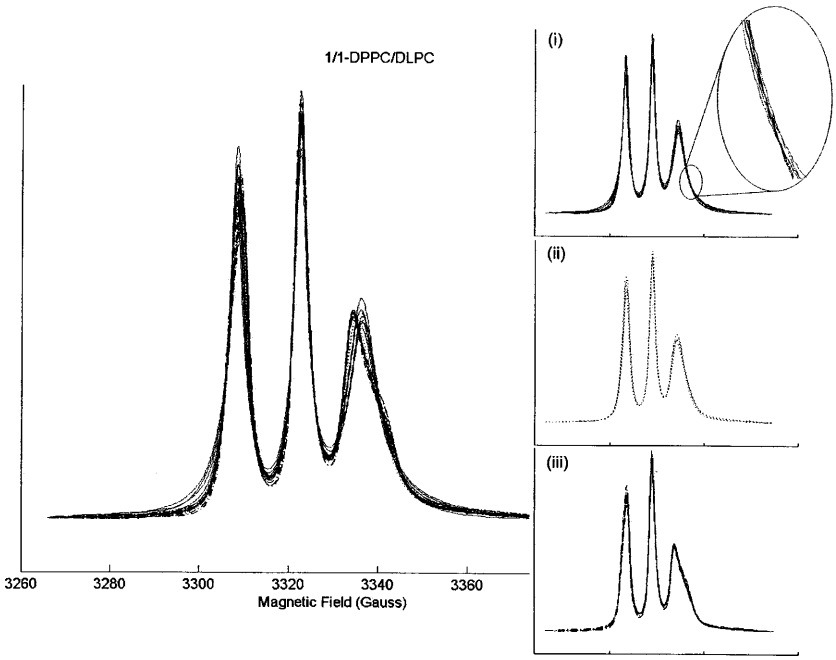

FIGURE 11 The absorption spectra for the DPPC/DLPC = 1/1 series with χ_{Chol} varying from 0.0 to 0.65. There is significant variation in the high field part of absorption peaks. The two segregated peaks are composed of $\chi_{Chol} = 0 \sim 0.127$, shown in *i* by solid lines, and $0.24 \sim 0.65$, shown in *iii* by dashed lines, respectively. The midrange shown in *ii* is for $\chi_{Chol} = 0.14 \sim 0.21$ (*dotted lines*). There are two boundaries located at $\chi_{Chol} = 0.127 \sim 0.14$ and $0.21 \sim 0.24$, which is consistent with fitting results. No isosbestic points exist in *i* since the sample trajectory is not along a tie-line.

agreement with those obtained by Ge et al. (1999) and Lou et al. (2001), where in the latter study we refer to their 9 GHz ESR results, analyzed in the same way as in our present study (see below).

Wolf and Chachaty (2000) used 7- and 16-doxylstearic spin-labeled fatty acids in lipid mixtures containing SM plus glycerophospholipids with and without cholesterol, and they observed a two-phase region. Based on spectral analysis, they found a gel-like SM region ($S_0 = 0.4$) and a fluid-like glycerophospholipid region ($S_0 = 0.1$), which is rendered a single component (with an in-between $S_0 = 0.27$ and increased motional rate) by addition of cholesterol. This is somewhat similar to the results for our trajectories wherein the DPPC/DLPC ratios were kept constant, whereas χ_{Chol} was varied. However, while the single phase we see at high χ_{Chol} (i.e., region *F*) has an increased motional rate, its ordering is significantly greater than either the L_α or L_β phases coexisting at lower χ_{Chol} (i.e., region *B*). In a related study by Veiga et al. (2001), they only provided a qualitative interpretation of their results with 14-PC in SM/PC/Chol, but inferred a cholesterol-poor L_β phase and cholesterol-rich L_o phase in coexistence at 4°C. Finally, we note that the saturating effect on ordering and dynamics with increased χ_{Chol} was clearly demonstrated in the studies of Shin and Freed (1989a,b) and Shin et al. (1990, 1993). This is consistent with our present observations on the L_o phase in the *F* region of the phase diagram.

It is of some significance to compare the present results with biological membranes. Ge et al. (1999) in their study of detergent-resistant membranes (DRM) from RBL-2H3 cells obtained results in good agreement with the two-component model system of DPPC/Chol 1:1, which according to Fig. 1 is in the L_o phase (region *F*). Our present results show that within region *F* at $\chi_{Chol} = 0.3$ there is not significant variation in S_0 and $R_\perp$ for 16-PC. Thus perhaps a range of compositions within region *F* could serve as a model system for these DRM. More recently Ge et al. (2003) have studied the plasma membrane vesicles derived from RBL-2H3 cells. Whereas other labels along the acyl chain (5-, 7-, and 10-PC) showed coexistence between two phases, ascribed to a L_o-like and L_α-like phase, those from 16-PC show only a single spectrum, which yields the values $S_0 = 0.17$ and $R_\perp = 2.5 \times 10^8\ s^{-1}$ at 24°C. This corresponds to a somewhat reduced ordering but comparable motional rate compared to the DRM ($S_0 = 0.23$, $R_\perp = 2.3 \times 10^8\ s^{-1}$) also at 24°C. It is not clear whether this is an average over an L_o-like and L_α-like phase (for which there is some evidence from 2D-ELDOR results; Y.-W. Chiang, A. Costa-Filho, and J. H. Freed, unpublished). Its S_0 and $R_\perp$ values do not precisely correspond to any compositions we found in this study of DPPC/DLPC/Chol ternary mixtures.

There are some caveats about the precise interpretation of the ESR dynamic and ordering parameters to which we wish to call attention. First of all, in the study by Lou et al. (2001) of 16-PC spectra at both 250 GHz and 9 GHz, they showed that the 9-GHz spectra are affected by both the faster internal dynamics of the ends of the acyl chains and the slower overall motions of the PC, with both types of motion constrained by the adjacent lipids. In the absence of results at different frequencies the simple MOMD fits to the 9-GHz spectra presented above, which do not distinguish between internal and overall dynamics, should be interpreted as simplified composites to the more complex dynamics. This is of particular importance in the analysis of the ordering tensor (i.e., S_0 and S_2), which in the MOMD analysis is a composite of the ordering tensors for internal and overall motions. Lou

et al. (2001) found that it is not generally possible to relate S_0 and S_2 that emerge from the MOMD analysis to the respective component ordering tensors for the two types of motion. In fact, they found from their multifrequency study for both pure DPPC and DPPC/Chol: 1/1 that the S_2 for just the acyl-chain internal ordering is close to zero, implying simple axial alignment, whereas the composite S_2 values obtained from the MOMD analysis were found to be substantial, as we have found in the present study.

Costa-Filho et al. (2003a,b) found that their 2D-ELDOR results at 17.3 GHz represent a somewhat different composite of both types of motions as compared to 9-GHz cw-ESR, and the greater sensitivity to the details of the dynamics of the former might allow the 2D-ELDOR spectra to be analyzed in terms of more sophisticated dynamical models. But for now, as Costa-Filho et al. (2003a,b) point out, this means that only a more qualitative comparison can be made between cw-ESR spectra and 2D-ELDOR spectra. In that spirit, they do report similar qualitative pictures emanating from the two types of spectroscopies, so we would expect the same to apply to a study of the present ternary system by 2D-ELDOR.

Isosbesticity concept

At present, the application of spectral grouping, as described in the previous section, plays a complementary (and not as definitive) role to simulation and spectral fitting in determining phase boundaries using spin-labeling ESR. In this context the isosbesticity concept was applied in this work for determining boundaries in a phase diagram. The first application of isosbesticity to ESR was in the context of hemoglobin studies (Ogawa and McConnell, 1967), as were further studies (Asakura et al., 1972; Ho et al., 1970; Ohnishi et al., 1968). Once the absorptivities of the component species become dependent on the external variables, isosbestic points do not occur (Marriott and Griffith, 1974). In addition, one requires that the spectra from the individual phases are not significantly affected by dynamic exchange between the phases. (For the nitroxide spectra in this study we estimate this translates into exchange rates $<\sim 10^7\ s^{-1}$.) Of course the isosbestic points may sometimes deviate from the fixed point due to experimental inaccuracy. In such circumstances, it is difficult to determine boundaries in the phase diagram by applying the isosbesticity concept. For researchers who lack access to spectral simulation, the use of spectral grouping and isosbestic points could be of value, but should be applied with extra care.

There are thus several challenges to using isosbesticity. In the present study, isosbestic points were reliably observed only in two-phase coexistence regions along a tie-line where the composition is varied, but the respective ESR lineshapes from each phase do not change. Furthermore an observed isosbestic point is meaningful only after the stacked absorption spectra are divided into categories by distinctive features in the absorption spectra. This is because there are significant spectral lineshape changes as a result of changes in molecular motion when the spin-bearing system studied is in the regime of slow motion (Freed, 1976). This can result in isosbestic-like points (e.g., the series $\chi_{Chol} = 0.3$ shown in Fig. 10 *C*). But more careful spectral grouping has enabled us to divide the spectra of the $\chi_{Chol} = 0.2$ trajectory into four categories (Fig. 10 *B*), although there were difficulties in assigning isosbestic points, since the tie-lines are unknown. On the other hand, the spectral peaks of $\chi_{Chol} = 0.3$ change continuously and more smoothly than $\chi_{Chol} = 0.2$, implying this is a one-phase trajectory with any ''isosbestic-like'' points due to lineshape changes. These direct observations on the absorption spectra are supported by the NLLS fits to these spectra, thereby reinforcing the assignments.

SUMMARY AND CONCLUSIONS

The dynamic structure of the various phases that exist and coexist over virtually the full range of composition for the ternary mixture of DPPC/DLPC/Chol has been mapped out using the end-chain spin-label 16-PC, which senses the molecular dynamical properties near the center of the membrane bilayer. This has been achieved by analysis of the cw-ESR spectra obtained over a wide range of compositions in terms of standard models of motional dynamics. This provides a detailed picture of the local rotational dynamics and ordering. It has proved successful because of the substantial variation of the ESR spectra as a function of composition despite the fact that the respective phases generally differ rather modestly from each other.

Typically, within a given phase there is not very significant variation in dynamic structure with composition. Exceptions are the substantial increase in ordering in the DLPC-rich L_α phase as cholesterol is added, and the initial increase in both ordering and motional rates for the L_o phase (the *F* region in Fig. 1) with addition of cholesterol, which, however, saturates out with further increase in cholesterol. The L_α and L_β phases are clearly distinguished by the very low ordering and more substantial motional rates of the former compared to the latter. The well-defined L_o phase (region *F*) exhibits the greatest ordering and fast motional rates comparable to, and even greater than, those of the L_α phase.

The spectral analysis also leads to determinations of phase boundaries characterized by abrupt changes in ordering and/or dynamical parameters as a function of composition. Phase boundaries found by ESR are typically in very good agreement with those previously found by Feigenson and Buboltz (2001) by other physical methods, which provide a more macroscopic (i.e., phenomenological) picture. There is, however, a complex region of the phase diagram (regions *D* and *E* in Fig. 1) wherein we observe new features. In particular, we find region *E* to involve two phases, which we nominally ascribe to an L_α and an L_o phase, but a further,

more-detailed study of this region of the phase diagram is recommended.

We have found that the ESR absorption spectra themselves, without spectral analysis, can provide a useful aid to the location of phase boundaries and to the existence of more than one coexisting phase. That is, abrupt spectral changes with just small changes in composition usually signal the onset of a phase change, whereas the existence of isosbestic points as a function of composition changes that follow a tie-line in the phase diagram implies coexistence of two phases.

Our analysis of the well-defined two-phase coexistence region (defined in Fig. 1 as region *B*) consisting of a DLPC-rich L_α phase and a DPPC-rich L_β phase is consistent with well-known thermodynamic requirements. The dynamic structural properties of these two phases do not change with composition within the coexistence region, but their relative amount does in accordance with the well-known lever rule. Application of the lever rule requires that the tie-lines within the coexistence region are known. Indeed it is well-defined in the region *B* at 0% cholesterol as the horizontal axis in Fig. 1. The other tie-lines in region *B* appear to be approximately parallel to this well-defined tie-line. A method is suggested to accurately determine tie-lines by ESR in future studies. In addition to tie-lines, accurate study of such two-phase regions requires knowledge of the partition coefficient of the spin-labeled molecule in the two phases. This is reliably determined to be close to unity for 16-PC along the 0% cholesterol tie-line, and this appears to be approximately true in other parts of region *B*. This marks 16-PC as a particularly useful probe for studies of coexisting phases, in addition to the fact that it exhibits substantially different ESR spectra in the different phases.

We thank Dr. Jeff Buboltz at Colgate University and Mr. Andrew K. Smith for their technical assistance of the sample preparation and ESR measurements.

Work was supported by National Science Foundation (MCB-0315330) and American Chemistry Society-Petroleum Research Fund (38464-AC71) to G.W.F; J.H.F. has been supported by grants from the National Institutes of Health/GM, National Institutes of Health/National Center for Research Resources and National Science Foundation/Chemistry. Computations were performed at the Cornell Theory Center. Y.S. has been partly supported by a grant (1185019) from the Japan Society for Promotion of Science.

REFERENCES

Alger, R. S. 1968. Electron Paramagnetic Resonance: Techniques and Applications. Interscience, New York. Chapt. 5.

Asakura, T., M. Shin, and M. Tamura. 1972. Enzymatic reduction of spin-labeled ferrihemoglobin. *J. Biol. Chem.* 247:3693–3694.

Atkins, P. W. 1998. Physical Chemistry. Freeman, New York. Chapt. 8.

Aussenac, F., M. Tavares, and E. J. Dufourc. 2003. Cholesterol dynamics in membranes of raft composition: a molecular point of view from ^{2}H and ^{31}P solid-state NMR. *Biochemistry.* 42:1383–1390.

Barnes, J. P., and J. H. Freed. 1998. Dynamics and ordering in mixed model membranes of dimyristoylphosphatidylcholine and dimyristoylphosphatidylserine: a 250-GHz electron spin resonance study using cholestane. *Biophys. J.* 75:2532–2546.

Borbat, P. P., A. J. Costa-Filho, K. A. Earle, J. K. Moscicki, and J. H. Freed. 2001. Electron spin resonance in studies of membranes and proteins. *Science.* 291:266–269.

Brown, D. A., and E. London. 1998. Functions of lipid rafts in biological membranes. *Annu. Rev. Cell Dev. Biomembr.* 14:111–136.

Brynesta, J., and G. P. Smith. 1968. Isosbestic points and internally linear spectra generated by changes in solvent composition or temperature. *J. Phys. Chem.* 72:296–300.

Buboltz, J. T., and G. W. Feigenson. 1999. A novel strategy for the preparation of liposomes: rapid solvent exchange. *Biochim. Biophys. Acta Biomembr.* 1417:232–245.

Budil, D. E., S. Lee, S. Saxena, and J. H. Freed. 1996. Nonlinear-least-squares analysis of slow-motion EPR spectra in one and two dimensions using a modified Levenberg-Marquardt algorithm. *J. Magn. Reson. A.* 120:155–189.

Cassol, R., M. T. Ge, A. Ferrarini, and J. H. Freed. 1997. Chain dynamics and the simulation of electron spin resonance spectra from oriented phospholipid membranes. *J. Phys. Chem. B.* 101:8782–8789.

Costa-Filho, A. J., R. H. Crepeau, P. P. Borbat, M. Ge, and J. H. Freed. 2003a. Lipid-gramicidin interactions: dynamic structure of the boundary lipid by 2D-ELDOR. *Biophys. J.* 84:3364–3378.

Costa-Filho, A. J., Y. Shimoyama, and J. H. Freed. 2003b. A 2D-ELDOR study of the liquid-ordered phase in multilamellar vesicle membranes. *Biophys. J.* 84:2619–2633.

Costa-Filho, A J., and J. H. Freed. 2003. Applications of 2D-FT-ESR to biological systems. The National Biomedical Center for Advanced ESR Technology (ACERT) Workshop on April 25, 2003, in Ithaca, NY.

Crepeau, R. H., S. Saxena, S. Lee, B. Patyal, and J. H. Freed. 1994. Studies on lipid membranes by two-dimensional Fourier transform ESR: enhancement of resolution to ordering and dynamics. *Biophys. J.* 66:1489–1504.

Demel, R. A., L. L. Vandeene, and B. A. Pethica. 1967. Monolayer interactions of phospholipids and cholesterol. *Biochim. Biophys. Acta.* 135:11–19.

Feigenson, G. W., and J. T. Buboltz. 2001. Ternary phase diagram of dipalmitoyl-PC/dilauroyl-PC/cholesterol: nanoscopic domain formation driven by cholesterol. *Biophys. J.* 80:2775–2788.

Freed, J. H. 1976. Theory of slow tumbling ESR spectra for nitroxides. *In* Spin Labeling: Theory and Applications. L. J. Berliner, editor. Academic Press, New York. 53–132.

Freed, J. H. 2000. New technologies in electron spin resonance. *Annu. Rev. Phys. Chem.* 51:655–689.

Freed, J. H., G. V. Bruno, and C. F. Polnaszek. 1971. Electron spin resonance lineshapes and saturation in the slow motional region. *J. Phys. Chem.* 75:3385–3399.

Gaffney, B. J., and D. Marsh. 1998. High-frequency, spin-label EPR of nonaxial lipid ordering and motion in cholesterol-containing membranes. *Proc. Natl. Acad. Sci. USA.* 95:12940–12943.

Ge, M., D. E. Budil, and J. H. Freed. 1994. An electron spin resonance study of interactions between phosphatidylcholine and phosphatidylserine in oriented membranes. *Biophys. J.* 66:1515–1521.

Ge, M., K. A. Field, R. Aneja, D. Holowka, B. Baird, and J. H. Freed. 1999. Electron spin resonance characterization of liquid-ordered phase of detergent-resistant membranes from RBL-2H3 cells. *Biophys. J.* 77:925–933.

Ge, M., and J. H. Freed. 1999. Electron-spin resonance study of aggregation of gramicidin in dipalmitoylphosphatidylcholine bilayers and hydrophobic mismatch. *Biophys. J.* 76:264–280.

Ge, M., A. Gidwani, H. A. Brown, D. Holowka, B. Baird, and J. H. Freed. 2003. Ordered and disordered phases coexist in plasma membrane vesicles of RBL-2H3 mast cells: an ESR study. *Biophys. J.* 85:1278–1288.

Ge, M. T., and J. H. Freed. 2003. Hydration, structure, and molecular interactions in the headgroup region of dioleoylphosphatidylcholine bilayers: an electron spin resonance study. *Biophys. J.* 85:4023–4040.

Gliss, C., O. Randel, H. Casalta, E. Sackmann, R. Zorn, and T. Bayerl. 1999. Anisotropic motion of cholesterol in oriented DPPC bilayers studied by quasielastic neutron scattering: the liquid-ordered phase. *Biophys. J.* 77:331–340.

Ho, C., J. J. Baldassa, and S. Charache. 1970. Electron paramagnetic resonance studies of spin-labeled hemoglobins and their implications to nature of cooperative oxygen binding to hemoglobin. *Proc. Natl. Acad. Sci. USA.* 66:722–729.

Huang, J. Y., and G. W. Feigenson. 1999. A microscopic interaction model of maximum solubility of cholesterol in lipid bilayers. *Biophys. J.* 76:A272.

Kar, L., E. Neyigner, and J. H. Freed. 1985. Electron-spin resonance and electron-spin-echo study of oriented multilayers of L-α-dipalmitoylphosphatidylcholine water-systems. *Biophys. J.* 48:569–595.

Kleemann, W., and H. M. McConnell. 1976. Interactions of proteins and cholesterol with lipids in bilayer membranes. *Biochim. Biophys. Acta.* 419:206–222.

Leathes, J. B. 1925. Role of fats in vital phenomena. *Lancet.* 208:852–856.

Livshits, V. A., and D. Marsh. 2000. simulation studies of high-field EPR spectra of spin-labeled lipids in membranes. *J. Magn. Reson.* 147:59–67.

Lou, Y., M. T. Ge, and J. R. Freed. 2001. A multifrequency ESR study of the complex dynamics of membranes. *J. Phys. Chem. B.* 105:11053–11056.

Marriott, T. B., and O. H. Griffith. 1974. Comments on isosbestic and isoclinic points in spin-labeling studies. *J. Magn. Reson.* 13:45–52.

McConnell, H. M. 1976. Molecular motion in biological membranes. *In* Spin Labeling: Theory and Applications. L. J. Berliner, editor. Academic Press, New York. 525–561.

Meirovitch, E., A. Nayeem, and J. H. Freed. 1984. Analysis of protein lipid interactions based on model simulations of electron-spin resonance-spectra. *J. Phys. Chem.* 88:3454–3465.

Miao, L., M. Nielsen, J. Thewalt, J. H. Ipsen, M. Bloom, M. J. Zuckermann, and O. G. Mouritsen. 2002. From lanosterol to cholesterol: structural evolution and differential effects on lipid bilayers. *Biophys. J.* 82:1429–1444.

Ogawa, S., and H. M. McConnell. 1967. Spin-label study of hemoglobin conformations in solution. *Proc. Natl. Acad. Sci. USA.* 58:19–26.

Ohnishi, S. I., T. Maeda, T. Ito, K. J. Hwang, and I. Tyuma. 1968. Spin-labeled hemoglobin subunits. *Biochemistry.* 7:2662–2666.

Pare, C., and M. Lafleur. 1998. Polymorphism of POPE/cholesterol system: a ^{2}H nuclear magnetic resonance and infrared spectroscopic investigation. *Biophys. J.* 74:899–909.

Polnaszek, C. F., and J. H. Freed. 1975. Electron spin resonance studies of anisotropic ordering, spin relaxation, and slow tumbling in liquid-crystalline solvents. *J. Phys. Chem.* 79:2283–2306.

Recktenwald, D. J., and H. M. McConnell. 1981. Phase equilibria in binary mixtures of phosphatidylcholine and cholesterol. *Biochemistry.* 20:4505–4510.

Rubenstein, J. L., B. A. Smith, and H. M. McConnell. 1979. Lateral diffusion in binary mixtures of cholesterol and phosphatidylcholines. *Proc. Natl. Acad. Sci. USA.* 76:15–18.

Schneider, D. J., and J. H. Freed. 1989. Calculating slow motional magnetic resonance spectra. A user's guide. *In* Spin Labeling: Theory and Application. J. Reuben, editor. Plenum, New York. 1–76.

Shimshick, E. J., and H. M. McConnell. 1973. Lateral phase separations in binary mixtures of cholesterol and phospholipids. *Biochem. Biophys. Res. Commun.* 53:446–451.

Shin, Y. K., D. E. Budil, and J. H. Freed. 1993. Thermodynamics and dynamics of phosphatidylcholine-cholesterol mixed model membranes in the liquid crystalline state: effects of water. *Biophys. J.* 65:1283–1294.

Shin, Y. K., and J. H. Freed. 1989a. Dynamic imaging of lateral diffusion by electron-spin resonance and study of rotational dynamics in model membranes: effect of cholesterol. *Biophys. J.* 55:537–550.

Shin, Y. K., and J. H. Freed. 1989b. Thermodynamics of phosphatidylcholine-cholesterol mixed model membranes in the liquid-crystalline state studied by the orientational order parameter. *Biophys. J.* 56:1093–1100.

Shin, Y. K., J. K. Moscicki, and J. H. Freed. 1990. Dynamics of phosphatidylcholine-cholesterol mixed model membranes in the liquid crystalline state. *Biophys. J.* 57:445–459.

Simons, K., and E. Ikonen. 1997. Functional rafts in cell membranes. *Nature.* 387:569–572.

Singer, S. J., and G. L. Nicolson. 1972. The fluid mosaic model of the structure of cell membranes. *Science.* 175:720–731.

Stockton, B. W., and I. C. P. Smith. 1976. A deuterium NMR study of the condensing effect of cholesterol on egg phosphatidylcholine bilayer membranes. *Chem. Phys. Lipids.* 17:251–261.

Tanaka, H., and J. H. Freed. 1984. Electron-spin resonance studies on ordering and rotational diffusion in oriented phosphatidylcholine multilayers—evidence for a new chain-ordering transition. *J. Phys. Chem.* 88:6633–6644.

Tardieu, A., V. Luzzati, and F. C. Reman. 1973. Structure and polymorphism of hydrocarbon chains of lipids—study of lecithin-water phases. *J. Mol. Biol.* 75:711–733.

Van Dijck, P. W. M., A. J. Laper, M. A. J. Oonk, and J. de Gier. 1977. Miscibility properties of binary phosphatidylcholine mixtures. *Biochim. Biophys. Acta.* 470:58–69.

Veiga, M. P., J. L. R. Arrondo, F. M. Goni, A. Alonso, and D. Marsh. 2001. Interaction of cholesterol with sphingomyelin in mixed membranes containing phosphatidylcholine, studied by spin-label ESR and IR spectroscopies. A possible stabilization of gel-phase sphingolipid domains by cholesterol. *Biochemistry.* 40:2614–2622.

Vist, M. R., and J. H. Davis. 1990. Phase-equilibria of cholesterol dipalmitoylphosphatidylcholine mixtures—^{2}H nuclear magnetic-resonance and differential scanning calorimetry. *Biochemistry.* 29:451–464.

Wolf, C., and C. Chachaty. 2000. Compared effects of cholesterol and 7-dehydrocholesterol on sphingomyelin-glycerophospholipid bilayers studied by ESR. *Biophys. Chem.* 84:269–279.

Wolf, C., K. Koumanov, B. Tenchov, and P. J. Quinn. 2001. Cholesterol favors phase separation of sphingomyelin. *Biophys. Chem.* 89:163–172.